Simulating bipartite quantum systems

Sanjeev Seahra*
Department of Mathematics and Statistics, University of New Brunswick, Fredericton, NB Canada E3B 5A3
(Dated: June 18, 2024)

We are interested in numerical simulations of the behaviour of various types of bipartite quantum systems with a focus on the behaviour of the entanglement entropy.

CONTENTS

I. COLLISION BETWEEN A PROJECTILE AND A DIATOMIC MOLECULE

A. Hamiltonian and Schrödinger equation

We consider a system described by a classical Hamiltonian

$$\mathcal{H} = \hbar\omega\left(\frac{p_x^2}{2m_1} + \frac{1}{2}m_1x^2 + \frac{p_y^2}{2m_2} + \lambda e^{x-y}\right), \tag{1}$$

where (x, p_x) and (y, p_y) are canonically conjugate pairs, respectively. All quantities within the round brackets are dimensionless, while ω is a frequency with dimensions of inverse time. Upon quantization, we may re-write the Hamiltonian as

$$\hat{H} = \hbar\omega(\hat{H}_1 + \hat{H}_2 + \lambda\hat{V}_1\hat{V}_2), \tag{2}$$

with

$$\hat{H}_1 = \frac{\hat{p}_x^2}{2m_1} + \frac{1}{2}m_1\hat{x}^2, \quad \hat{H}_2 = \frac{\hat{p}_y^2}{2m_2}, \quad \hat{V}_1 = e^{\hat{x}}, \quad \hat{V}_2 = e^{-\hat{y}}. \tag{3}$$

Physically, this system represents a diatomic molecule (subsystem 1) and a projectile (subsystem 2). The x coordinate represents the separation between the two atoms in the molecule, while y represents the separation between the projectile and the molecule.

We now use units in which $\hbar = 1$. Upon quantization, the Schrödinger equation for the system is

$$i\frac{\partial\psi}{\partial\tau} = -\frac{1}{2m_1}\frac{\partial^2\psi}{\partial x^2} + \frac{1}{2}m_1x^2\psi - \frac{1}{2m_2}\frac{\partial^2\psi}{\partial y^2} + \lambda e^{x-y}\psi, \quad (x, y) \in \mathbb{R}^2, \tag{4}$$

where $\tau = \omega t$.

* sseahra@unb.ca

B. Method of lines discretization and Crank-Nicholson stencil

In order to solve the Schrödinger equation numerically using the method of lines, we consider a finite computational domain and Dirichlet boundary conditions:

$$\Omega = \left\{(x,y) \in \left[-\tfrac{1}{2}L_1, \tfrac{1}{2}L_1\right] \times \left[-\tfrac{1}{2}L_2, \tfrac{1}{2}L_2\right]\right\}, \quad \psi\big|_{\partial\Omega} = 0. \tag{5}$$

Now, suppose that we discretize the x and y directions such that

$$x \mapsto \{x_0 = -\tfrac{1}{2}L_1, x_1, x_2 \ldots x_n, x_{n+1} = \tfrac{1}{2}L_1\}, \quad x_{i+1} - x_i = h_x = L_1/(n+1), \tag{6}$$

$$y \mapsto \{y_0 = -\tfrac{1}{2}L_2, y_1, y_2 \ldots y_m, y_{m+1} = \tfrac{1}{2}L_2\}, \quad y_{j+1} - y_j = h_y = L_2/(m+1). \tag{7}$$

The Dirichlet boundary conditions then read

$$\psi(\tau, x_0, y) = \psi(\tau, x_{n+1}, y) = \psi(\tau, x, y_0) = \psi(\tau, x, y_{m+1}) = 0. \tag{8}$$

We can define an $n \times m$ matrix $\Psi(\tau)$ whose entries are numeric approximations to $\psi(\tau, x, y)$ evaluated at the interior xy-gridpoints

$$\Psi(\tau) \in \mathbb{C}^{n\times m}, \quad \Psi_{ij}(\tau) \approx \psi(\tau, x_i, y_j). \tag{9}$$

Then the Schrödinger equation may be approximated as

$$i\frac{d\Psi}{d\tau} = \frac{1}{2m_1}P_x^2\Psi + \frac{1}{2m_2}\Psi P_y^2 + \frac{1}{2}m_1 X^2\Psi + \lambda U_x \Psi U_y. \tag{10}$$

where $H_x, X \in \mathbb{R}^{n\times n}$ and $H_y, Y \in \mathbb{R}^{m\times m}$ such that

$$P_x^2 = -\frac{1}{h_x^2}\begin{pmatrix} -2 & 1 & & \\ 1 & -2 & 1 & \\ & 1 & -2 & 1 \\ & & & \ddots \end{pmatrix}, \quad P_y^2 = -\frac{1}{h_y^2}\begin{pmatrix} -2 & 1 & & \\ 1 & -2 & 1 & \\ & 1 & -2 & 1 \\ & & & \ddots \end{pmatrix},$$

$$X = \begin{pmatrix} x_1 & & & \\ & x_2 & & \\ & & \ddots & \\ & & & x_n \end{pmatrix}, \quad U_x = \begin{pmatrix} e^{x_1} & & & \\ & e^{x_2} & & \\ & & \ddots & \\ & & & e^{x_m} \end{pmatrix}, \quad U_y = \begin{pmatrix} e^{-y_1} & & & \\ & e^{-y_2} & & \\ & & \ddots & \\ & & & e^{-y_m} \end{pmatrix}. \tag{11}$$

This can be recast into the standard form for a system of $n \times m$ of linear first order differential equations by defining the "vectorization" $\vec{\Psi}$ of Ψ:

$$\vec{\Psi} = \mathrm{vec}\,(\Psi). \tag{12}$$

Basically, $\vec{\Psi}$ is the $n \times m$ dimensional column vector formed by stacking the columns of Ψ on top of one another. Then, we have

$$\frac{d\vec{\Psi}}{d\tau} = A\vec{\Psi}, \tag{13}$$

where

$$A = -i\left[\frac{1}{2m_1}(I_m \otimes P_x^2) + \frac{1}{2}m_1(I_m \otimes X^2) + \frac{1}{2m_2}(P_y^2 \otimes I_n) + \lambda(U_y \otimes U_x)\right]. \tag{14}$$

Here, I_n and I_m are n and m dimensional identity matrices, respectively, and $\otimes$ represents the matrix Kronecker product. (We have made use of the fact that all matrices are symmetric.) The matrix ODE can then be solved numerically by introducing a time discretization $\tau \mapsto \{\tau_k\}$ with $\tau_{k+1} - \tau_k = s$. The Crank-Nicholson stencil for solving the system is then

$$\left(I_{nm} - \tfrac{1}{2}sA\right)\vec{\Psi}_{k+1} = \left(I_{nm} + \tfrac{1}{2}sA\right)\vec{\Psi}_k, \quad \vec{\Psi}(\tau_k) \approx \vec{\Psi}_k. \tag{15}$$

Suppose we want to calculate the expectation value of some phase space function of x and $p(x)$; i.e. $f(x, p_x)$. Due to linearity, the action of the associated operator $\hat{f}$ on the wavefunction will be approximated by a left-acting linear map on the Ψ matrix

$$(\hat{f}\psi)(\tau, x_i, y_j) \approx \sum_{i'} F_{ii'} \Psi_{i'j}, \tag{16}$$

for some matrix F. Hence, we can approximate the expectation value as

$$\langle f(x, p_x) \rangle = \iint dx\, dy\, \psi^*(\tau, x, y)(\hat{f}\psi)(\tau, x, y) \approx \sum_{ii'j} h_x h_y \Psi^*_{ij} F_{ii'} \Psi_{i'j} = \mathrm{Tr}\,[\rho_1 F], \tag{17}$$

where the reduced density matrix for the x-sector is

$$\rho_1 = h_x h_y \Psi \Psi^\dagger. \tag{18}$$

Similarly, the reduced density matrix for the y-sector is

$$\rho_2 = h_x h_y \Psi^{\mathrm{T}} \Psi^*. \tag{19}$$

Explicitly, expectation values and variances of x and y are given by

$$\langle x \rangle = \mathrm{Tr}\,(\rho_1 X), \quad \mathrm{Var}(x) = \sqrt{\mathrm{Tr}\,(\rho_1 X^2) - \langle x \rangle^2}, \quad \langle y \rangle = \mathrm{Tr}\,(\rho_2 Y), \quad \mathrm{Var}(y) = \sqrt{\mathrm{Tr}\,(\rho_2 Y^2) - \langle y \rangle^2} \tag{20}$$

Once we have the reduced density matrices, the von Neumann entanglement entropy can be obtained by calculuating the eigenvalues $\{\Lambda_i\}$ of either ρ_1 or ρ_2, and then computing the sum

$$S_{\mathrm{VN}} = -\sum_i \Lambda_i \ln \Lambda_i. \tag{21}$$

Note that since the density matrices are themselves functions of time, the above expectation values and entanglement entropy are also functions of time.

C. Solution of the Schrödinger equation via subsystem Hamiltonian eigenbasis expansion

We assume that the energy eigenvalue problem for each of the subsystem Hamiltonians is easily solvable:

$$\hat{H}_1 |\mu\rangle = E_\mu |\mu\rangle, \quad \hat{H}_2 |\nu\rangle = E_\nu |\nu\rangle. \tag{22}$$

In this section, we work in a finite truncation where we keep the d_1 and d_2 lowest energy eigenstatues of subsystem 1 (the oscillator) and subsystem 2 (the projectile), respectively. Our notation is such that the indices $\mu, \mu' = 0, 1, 2 \ldots d_1 - 1$ will always be associated with subsystem 1 and the indices $\nu, \nu' = 1, 2 \ldots d_2$ will always be associated with subsystem 2.[1] Then, a complete basis for the total Hilbert space is given by the $d_1 \times d_2$ basis states

$$|\mu, \nu\rangle = |\mu\rangle \otimes |\nu\rangle, \quad \langle \mu', \nu' | \mu, \nu \rangle = \delta_{\mu\mu'} \delta_{\nu\nu'}. \tag{23}$$

We write the full state vector of the system in the Schrödinger representation as

$$|\psi(\tau)\rangle = \sum_{\mu\nu} z_{\mu,\nu}(\tau) |\mu, \nu\rangle. \tag{24}$$

Inserting this into the Schrödinger equation

$$i\partial_\tau |\psi(\tau)\rangle = \hat{H} |\psi(\tau)\rangle \tag{25}$$

---

[1] The slightly odd indexing conventions for the two subsystems will be for later convenience.

yields

$$i\partial_\tau z_{\mu',\nu'}(\tau) = \sum_{\mu\nu} \langle \mu', \nu' | \hat{H} | \mu, \nu \rangle z_{\mu,\nu}(\tau). \tag{26}$$

We organize the expansion coefficients into a matrix:

$$Z(\tau) = \begin{pmatrix} z_{0,1}(\tau) & z_{0,2}(\tau) & \cdots & z_{0,d_2}(\tau) \\ z_{1,1}(\tau) & z_{1,2}(\tau) & \cdots & z_{1,d_2}(\tau) \\ \vdots & \vdots & \ddots & \vdots \\ z_{d_1-1,1}(\tau) & z_{d_1-1,2}(\tau) & \cdots & z_{d_1-1,d_2}(\tau) \end{pmatrix}.$$

Inserting the expansion (24) into the Schrodinger equation yields:

$$i\partial_\tau Z = H_1 Z + Z H_2 + \lambda V_1 Z V_2^{\mathrm{T}}, \tag{27}$$

where the H_1, H_2, V_1, and V_2 square matrices have entries

$$\begin{aligned} (H_1)_{\mu'\mu} &= \langle \mu' | \hat{H}_1 | \mu \rangle, & (V_1)_{\mu'\mu} &= \langle \mu' | \hat{V}_1 | \mu \rangle, \\ (H_2)_{\nu'\nu} &= \langle \nu' | \hat{H}_2 | \nu \rangle, & (V_2)_{\nu'\nu} &= \langle \nu' | \hat{V}_2 | \nu \rangle. \end{aligned} \tag{28}$$

Note that since $|\mu\rangle$ and $|\nu\rangle$ are eigenvectors of $\hat{H}_1$ and $\hat{H}_2$, respectively, H_1 and H_2 are real diagonal matrices. Furthermore, V_1 and V_2 are Hermitian matrices due to the self-adjointness of the associated operators. Equation (27) represents $d_1 \times d_2$ complex linear differential equations whose solutions completely specify the quantum dynamics of the system. In addition to the above, other useful matrices are the representations of $\hat{x}$, $\hat{x}^2$, etc., in the respective eigenbases of $\hat{H}_1$, and $\hat{H}_2$. These will have matrix elements of the form

$$\begin{aligned} (X^k)_{\mu'\mu} &= \langle \mu' | \hat{x}^k | \mu \rangle, & (P_x^k)_{\mu'\mu} &= \langle \mu' | \hat{p}_x^k | \mu \rangle, \\ (Y^k)_{\nu'\nu} &= \langle \nu' | \hat{y}^k | \nu \rangle, & (P_y^k)_{\nu'\nu} &= \langle \nu' | \hat{p}_y^k | \nu \rangle. \end{aligned} \tag{29}$$

with $k = 1, 2 \ldots$

For the oscillator, the energy eigenvectors are the familiar Fock states for the simple harmonic oscillator. It is useful to define raising and lowering operators by

$$\hat{a} = \frac{m_1^{1/2}\hat{x} + i m_1^{-1/2}\hat{p}}{\sqrt{2}}, \quad \hat{a}^\dagger = \frac{m_1^{1/2}\hat{x} - i m_1^{-1/2}\hat{p}}{\sqrt{2}} \tag{30}$$

which implies that

$$[\hat{a}, \hat{a}^\dagger] = 1, \quad \hat{H}_1 = \hat{a}^\dagger \hat{a} + \tfrac{1}{2}. \tag{31}$$

Hamiltonian eigenstates satisfy

$$\hat{H}_1 |\mu\rangle = (\mu + \tfrac{1}{2})|\mu\rangle, \quad \mu = 0, 1, 2, \ldots \tag{32}$$

The coordinate representation of the eigenfunctions is

$$\chi_\mu(x) = \langle x | \mu \rangle = \frac{1}{\sqrt{2^\mu \mu!}} \left(\frac{m_1}{\pi}\right)^{1/4} e^{-m_1 x^2/2} H_\mu(\sqrt{m_1} x), \tag{33}$$

where H_μ is a Hermite polynomial. From this we can obtain

$$X = \frac{1}{\sqrt{2m_1}} \begin{pmatrix} 0 & \sqrt{1} & & \\ \sqrt{1} & 0 & \sqrt{2} & \\ & \sqrt{2} & 0 & \\ & & & \ddots \end{pmatrix}, \; P = -i\sqrt{\frac{m_1}{2}} \begin{pmatrix} 0 & +\sqrt{1} & & \\ -\sqrt{1} & 0 & +\sqrt{2} & \\ & -\sqrt{2} & 0 & \\ & & & \ddots \end{pmatrix}, \; H_1 - \frac{1}{2} I = \begin{pmatrix} 0 & & & \\ & 1 & & \\ & & 2 & \\ & & & \ddots \end{pmatrix}, \tag{34}$$

and I is the identity matrix. The V_1 matrix can be shown to have elements

$$(V_1)_{\mu\mu'} = (V_1)_{\mu'\mu} = e^{1/4m_1} (2m_1)^{-(\mu-\mu')/2} \sqrt{\frac{\mu'!}{\mu!}} \, L_{\mu'}^{\mu-\mu'} \left(-\frac{1}{2m_1}\right), \quad \mu \geq \mu', \tag{35}$$

where $L_{\mu'}^{\mu-\mu'}$ are generalized Laguerre polynomials.

For the projectile, the above matrix elements can be written out explicitly if we note that a complete basis of eigenfunctions (written in the standard coordinate representation is):

$$\phi_\nu(y) = \langle y|\nu\rangle = \sqrt{\frac{2}{L_2}} \sin\left[\frac{\nu\pi}{2}\left(\frac{2y}{L_2}+1\right)\right]. \tag{36}$$

We then have

$$(H_2)_{\nu'\nu} = \frac{\nu^2\pi^2}{2m_2L_2^2}\delta_{\nu\nu'}, \qquad (V_2)_{\nu'\nu} = \frac{4\pi^2 L_2\nu\nu'[e^{L_2/2}-(-1)^{\nu+\nu'}e^{-L_2/2}]}{[L_2^2+\pi^2(\nu+\nu')^2][L_2^2+\pi^2(\nu-\nu')^2]},$$

$$(Y)_{\nu'\nu} = \begin{cases} \dfrac{4L_2\nu\nu'[(-1)^{\nu+\nu'}-1]}{\pi^2(\nu-\nu')^2(\nu+\nu')^2} & \text{for } \nu\neq\nu', \\ 0 & \text{for } \nu=\nu', \end{cases} \qquad (P_y)_{\nu'\nu} = \begin{cases} i\dfrac{2\nu\nu'[(-1)^{\nu+\nu'}-1]}{L_2(\nu'^2-\nu^2)} & \text{for } \nu\neq\nu', \\ 0 & \text{for } \nu=\nu', \end{cases}$$

$$(Y^2)_{\nu'\nu} = \begin{cases} \frac{4L_2^2\nu\nu'[(-1)^{\nu+\nu'}+1]}{\pi^2(\nu-\nu')^2(\nu+\nu')^2} & \text{for } \nu\neq\nu', \\ \frac{L_2^2(\pi^2\nu^2-6)}{12\nu^2\pi^2} & \text{for } \nu=\nu', \end{cases} \qquad (P_y^2)_{\nu'\nu} = \frac{\nu^2\pi^2}{L_2^2}\delta_{\nu\nu'}.$$

II. TEST CASE

A suitable test case for both the Crank-Nicholson method and the eigenbasis expansion method involves real space initial data for the wavefunction to be a product of the ground state oscillator wavefunction times a Gaussian wavepacket for the projectile with initial position and velocity y_0 and p_0, respectively.

$$\psi(0,x,y) = \mathcal{N}\chi_0(x)e^{ip_0y}\exp\left[-\frac{(y-y_0)^2}{4\sigma^2}\right], \tag{37}$$

where

$$\chi_0(x) = \frac{m_1^{1/4}}{\pi^{1/4}}e^{-m_1x^2/2}, \tag{38}$$

and $\mathcal{N}$ is a normalization factor

$$\mathcal{N} = \left\{\int_{-L_2}^{L_2} dy\, \exp\left[-\frac{(y-y_0)^2}{2\sigma^2}\right]\right\}^{-1/2}, \tag{39}$$

which could be expressed in terms of an error function if desired. For the eigenbasis method, initial data for $z_{\mu\nu}$ will be

$$z_{\mu\nu}(0) = \delta_{\mu,0}c_\nu, \quad c_\nu = \mathcal{N}\sqrt{\frac{2}{L_2}}\int_{-L_2}^{L_2} dy \sin\left[\frac{\nu\pi}{2}\left(\frac{2y}{L_2}+1\right)\right]e^{ip_0y}\exp\left[-\frac{(y-y_0)^2}{4\sigma^2}\right]. \tag{40}$$

For the test case, we will take parameters

$$\lambda = 1, \quad m_1 = 1, \quad m_2 = 1, \quad y_0 = 10, \quad p_0 = -1, \quad \sigma = 3. \tag{41}$$

These parameters are fundamental, but there are additional "nuisance" parameters that must be selected in order for either numerical scheme to run. Some suggested values are

$$L_1 = 10, \quad L_2 = 50, \quad d_1 = 10, \quad d_2 = 40, \quad \tau \in [0,20]. \tag{42}$$

It may be necessary to adjust these to get reasonable results.

III. PLOTS FROM DOYEON

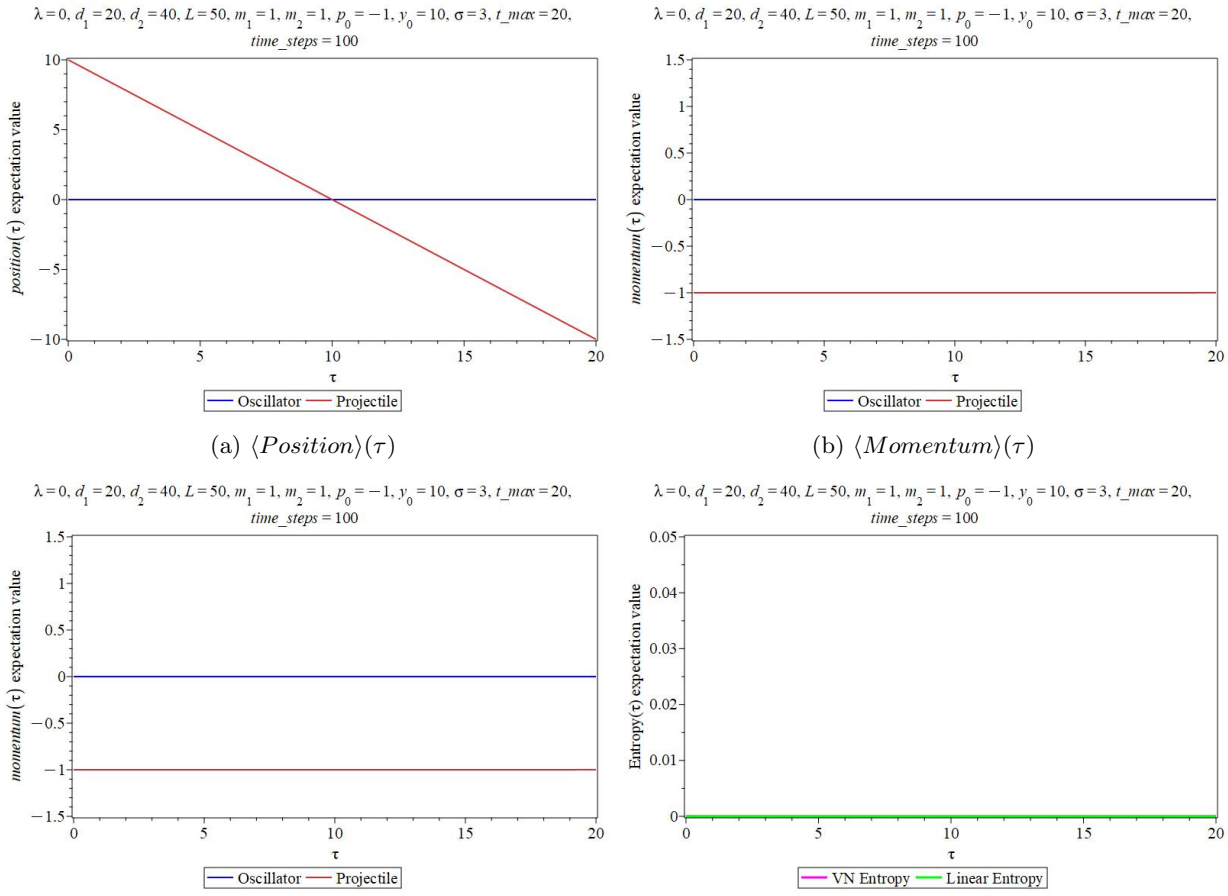

(a) $\langle Position \rangle(\tau)$ (b) $\langle Momentum \rangle(\tau)$

(c) $\langle Energy \rangle(\tau)$ (d) $\langle Entropy \rangle(\tau)$

FIG. 1: $\lambda = 0$, $y_0 = 10$

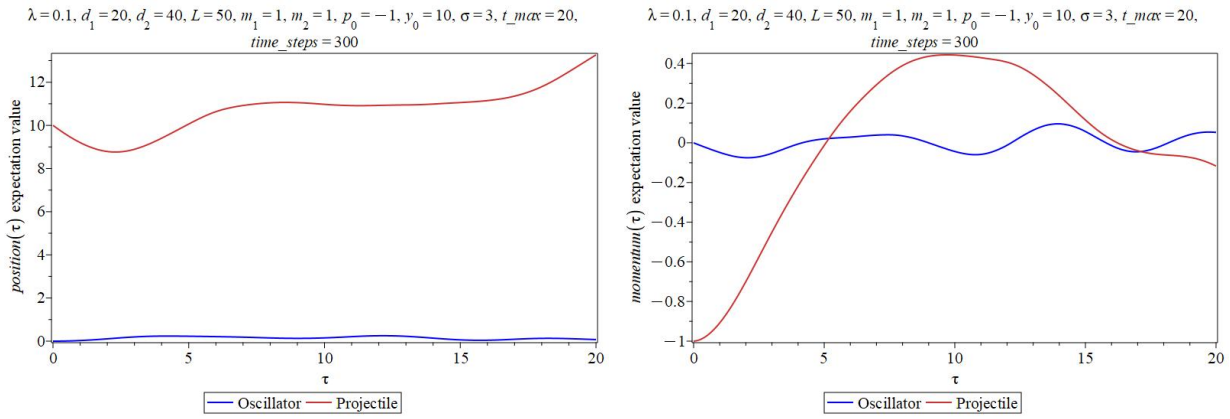

(a) $\langle Position \rangle(\tau)$

(b) $\langle Momentum \rangle(\tau)$

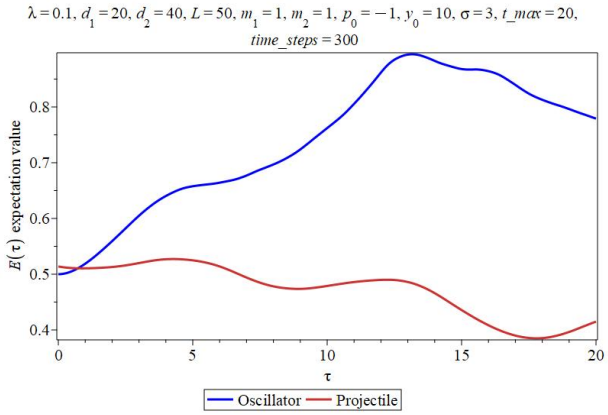

(c) $\langle Energy \rangle(\tau)$

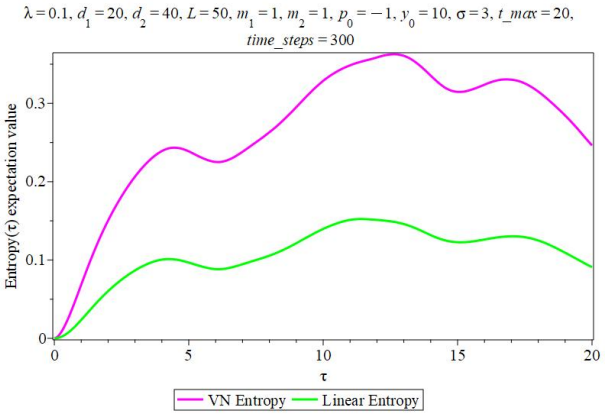

(d) $\langle Entropy \rangle(\tau)$

FIG. 2: $\lambda = 0.1$, $y_0 = 10$

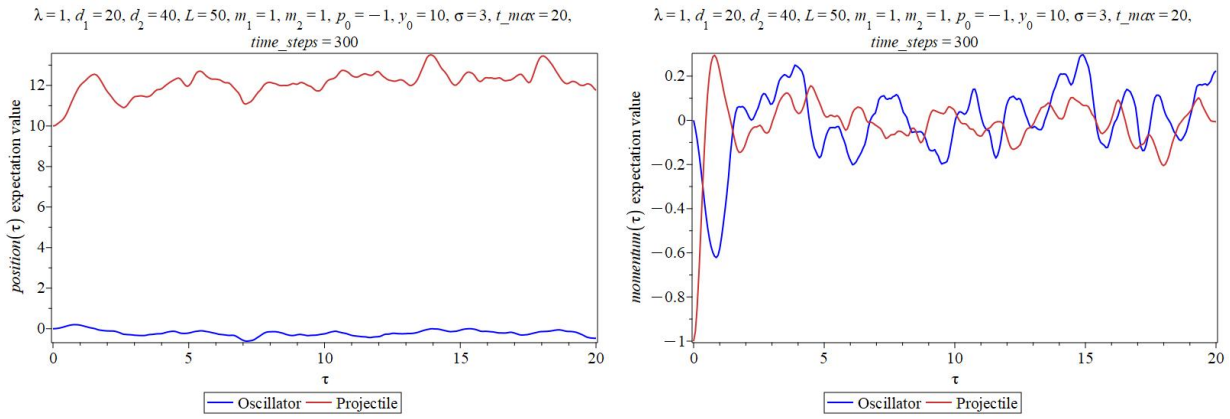

(a) $\langle Position \rangle(\tau)$

(b) $\langle Momentum \rangle(\tau)$

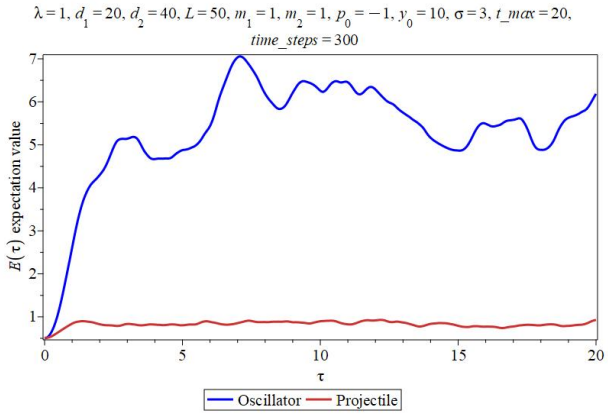

(c) $\langle Energy \rangle(\tau)$

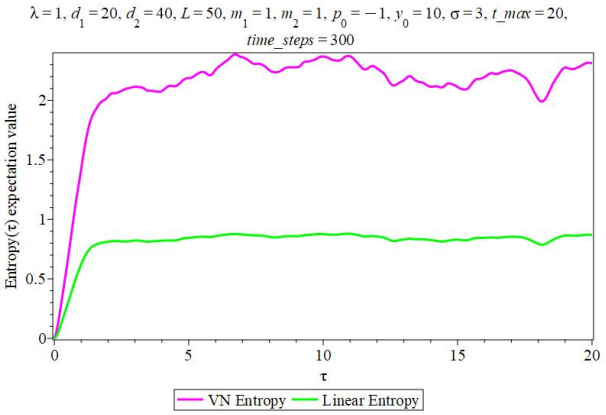

(d) $\langle Entropy \rangle(\tau)$

FIG. 3: $\lambda = 1$, $y_0 = 10$

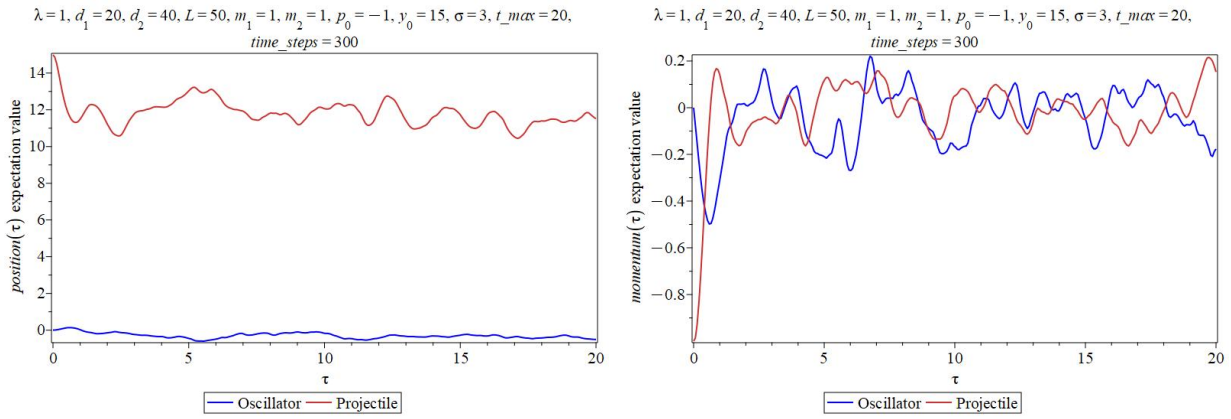

(a) $\langle Position \rangle(\tau)$

(b) $\langle Momentum \rangle(\tau)$

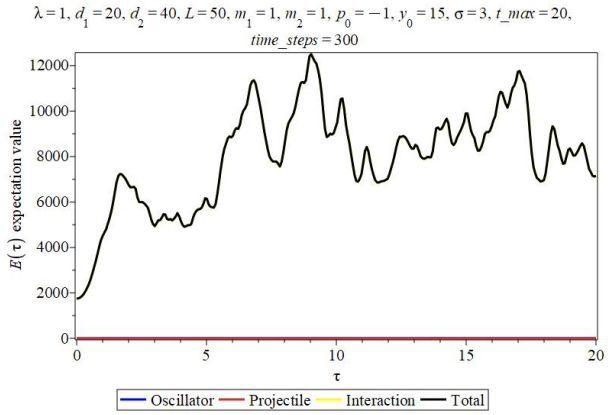

(c) $\langle Energy \rangle(\tau)$

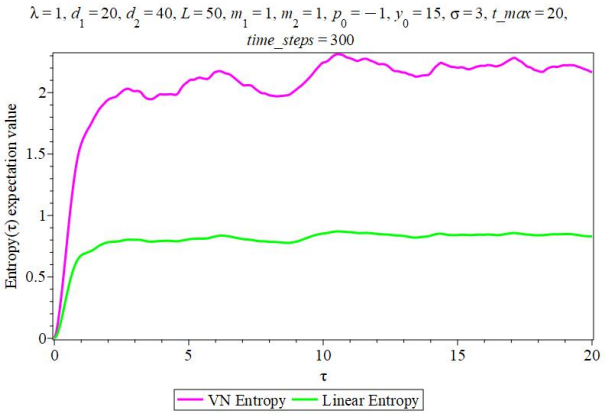

(d) $\langle Entropy \rangle(\tau)$

FIG. 4: $\lambda = 1$, $y_0 = 15$, in (c) the yellow line(/the red line) overlapped in the black line(/the blue line)

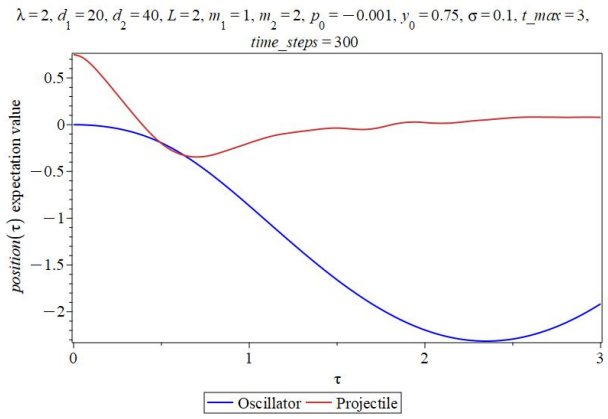

(a) $\langle Position \rangle(\tau)$

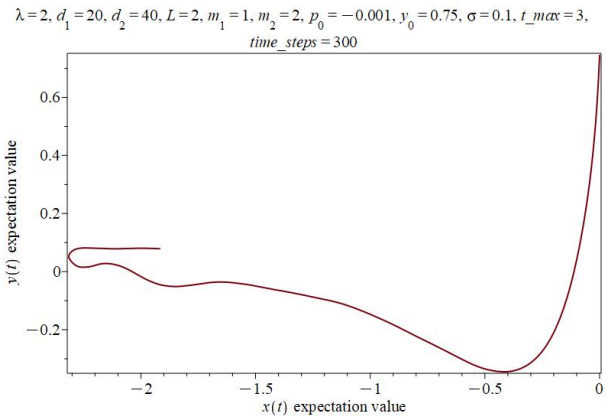

(b) xy plot

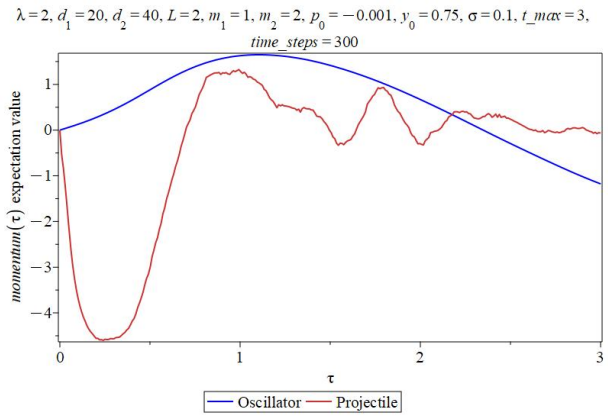

(c) $\langle Momentum \rangle(\tau)$

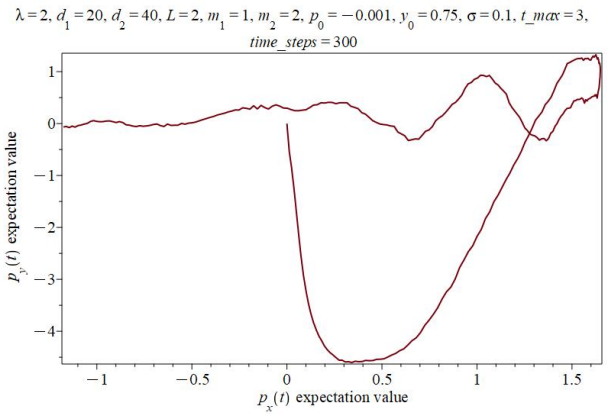

(d) $p_x p_y$ plot

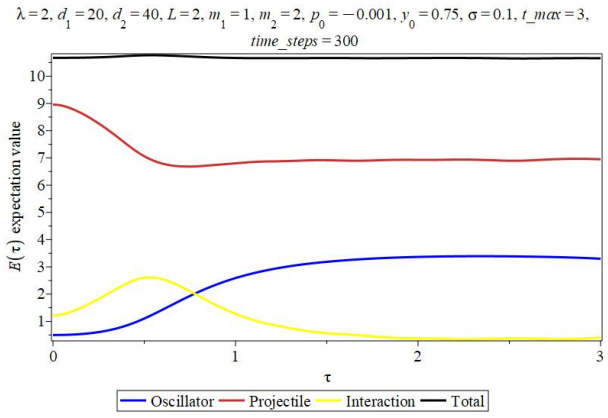

(e) $\langle Energy \rangle(\tau)$

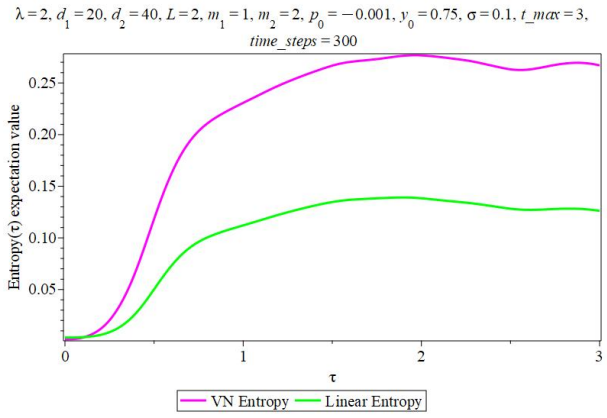

(f) $\langle Entropy \rangle(\tau)$

FIG. 5: $L = 2$

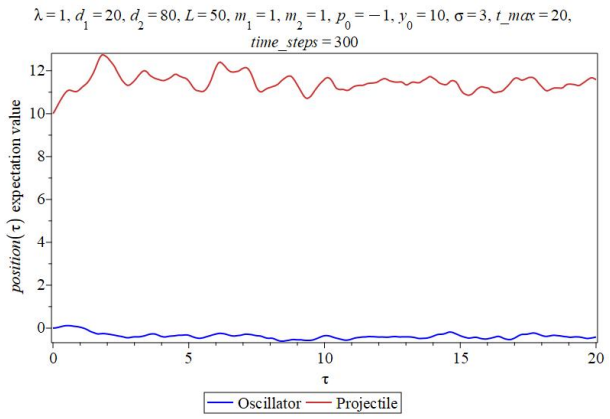

(a) $\langle Position \rangle(\tau)$

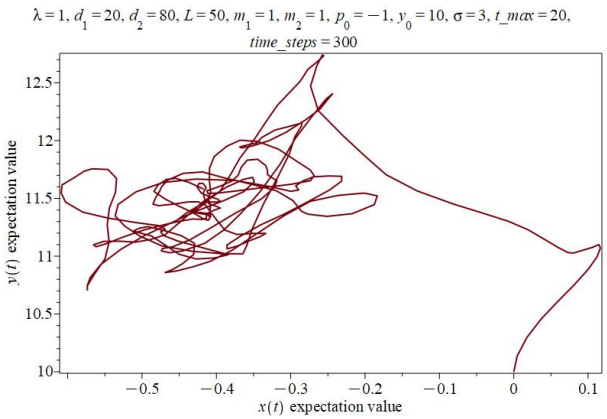

(b) xy plot

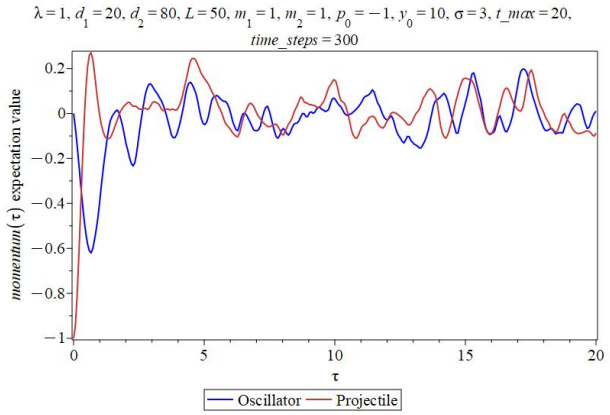

(c) $\langle Momentum \rangle(\tau)$

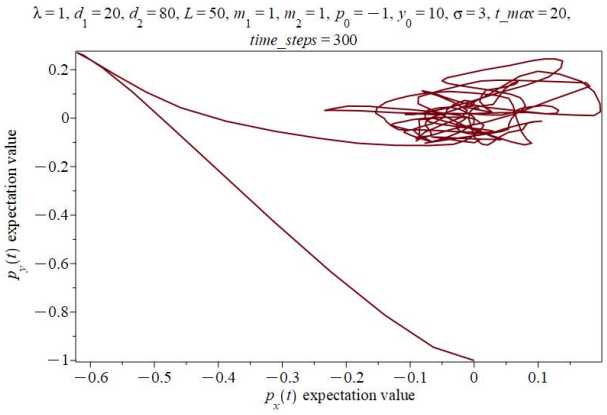

(d) $p_x p_y$ plot

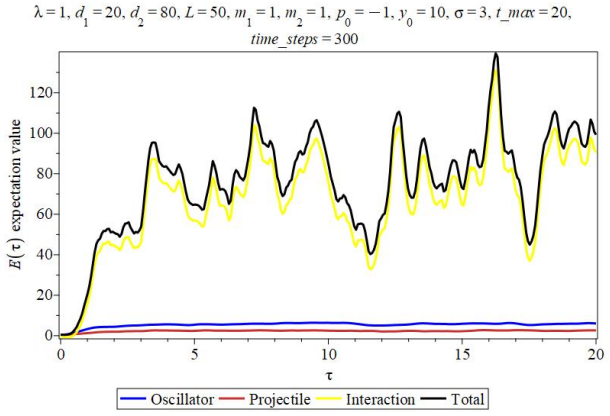

(e) $\langle Energy \rangle(\tau)$

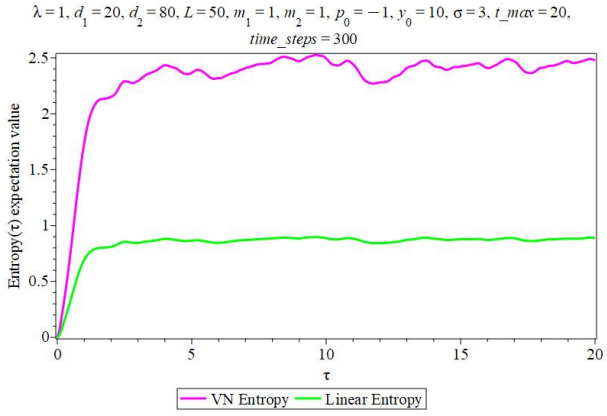

(f) $\langle Entropy \rangle(\tau)$

FIG. 6: $d2 = 80$

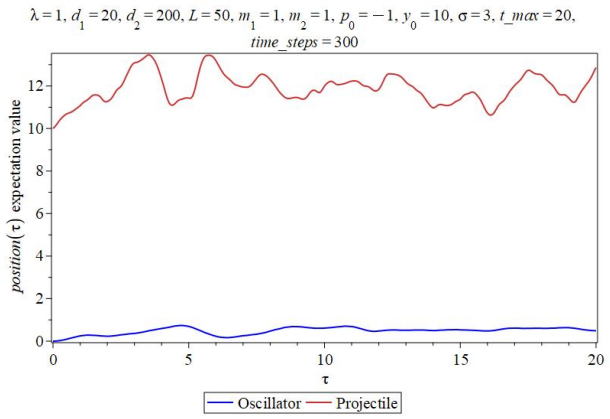

(a) $\langle Position \rangle(\tau)$

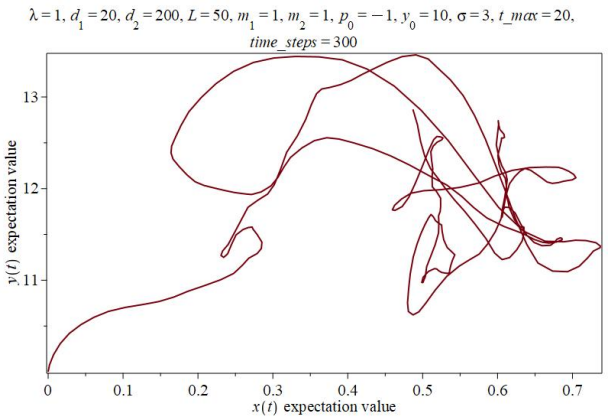

(b) xy plot

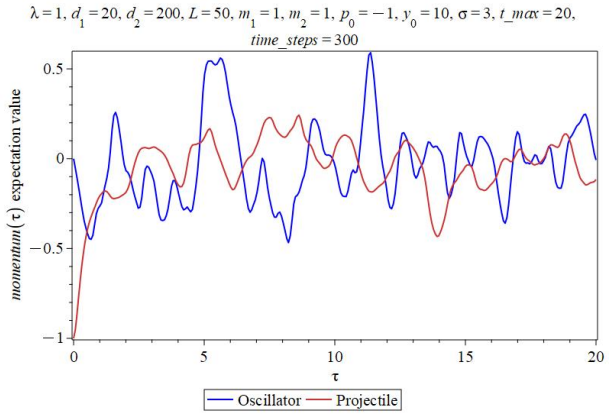

(c) $\langle Momentum \rangle(\tau)$

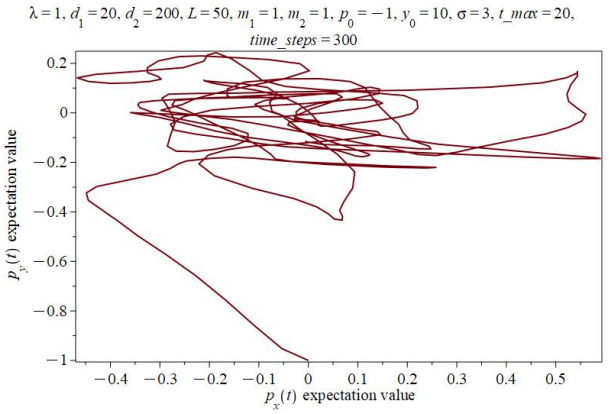

(d) $p_x p_y$ plot

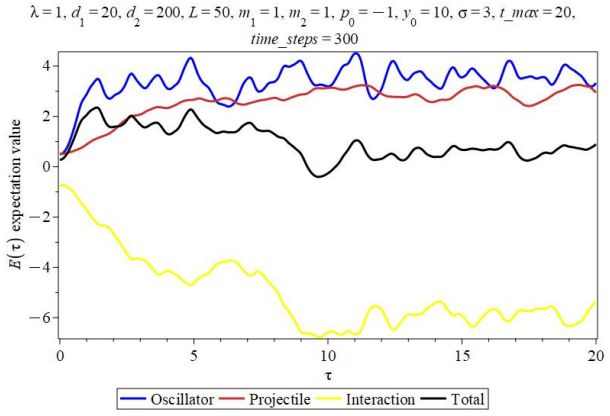

(e) $\langle Energy \rangle(\tau)$

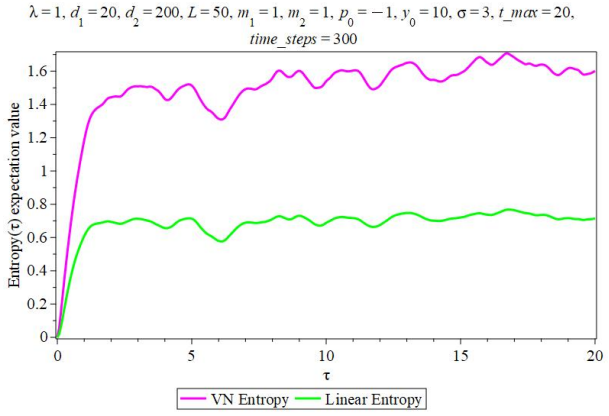

(f) $\langle Entropy \rangle(\tau)$

FIG. 7: $d2 = 200$

IV. PLOTS FROM GAIA

A. Introduction

This section shall be a working section to include any plots and work that I do over time. This will all be produced using either the main Python file on the Digital Research Alliance of Canada, or locally through a Jupyter (ipynb) notebook. All of this code will align with a public GitHub that I will update regularly. **This GitHub also includes videos for everything here, showing the wave evolution.** It can be found at the following address:

https://github.com/gaianoseworthy/CN_Schrodinger.

Furthermore, whenever the Hamiltonian is calculated, it is done so using the following method:

```
X2 = np.diag(np.vectorize(lambda x : x**2)(x))
Px = (-1/(hx**2))*sps.diags([1, -2, 1], [-1, 0, 1], shape=(n, n))
HPx = (1/(2*1)) * (Px**2) + (1/)*X2
observables[i,3] = np.real(np.trace(np.matmul(HPx, rho1)))
```

B. Ground State 100x5000x1000

In this section, and really all future sections, the initial wavefunction will be set to avoid the extreme oscillations initially. The wavefunction is:

$$\Psi_0(x,y,t) = e^{-i(v_x x - v_y y)} e^{-\frac{(y-y_0)^2}{4\sigma_y^2}} \frac{1}{\sqrt{2}\pi^4} e^{-\frac{x^2}{2}}$$

It will also use the following initial variables:

- $x \in [-10, 10], m = 100$
- $y \in [-10, 90], n = 500$
- $t \in [0, 250], N = 1000$
- $x_0 = 0, y_0 = 75$
- $v_x = 0, v_y = -1$
- $\sigma_y = 1$
- $\lambda = 1$

This produces the following result:

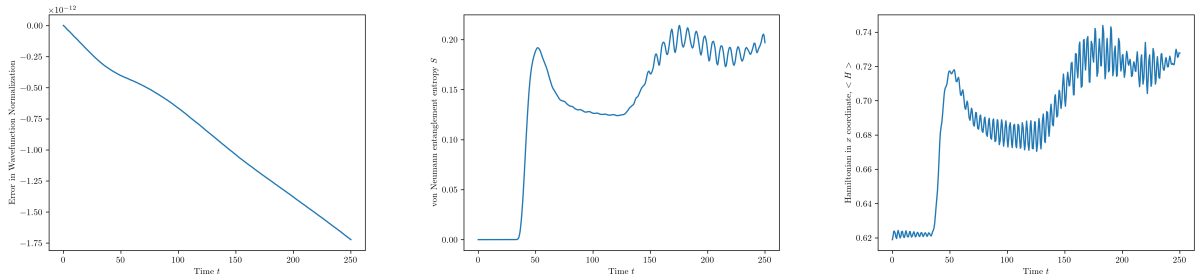

FIG. 8: Normalization, Entropy, and Hamiltonian of the 100x5000x1000 test with non-gound state initial Gaussian conditions.

C. Low Lambda 100x5000x2000

Another interesting question is what if we set *lambda* to some low number, such as 0.01, with the new ground state wavefunction? Well, these results are as follows:

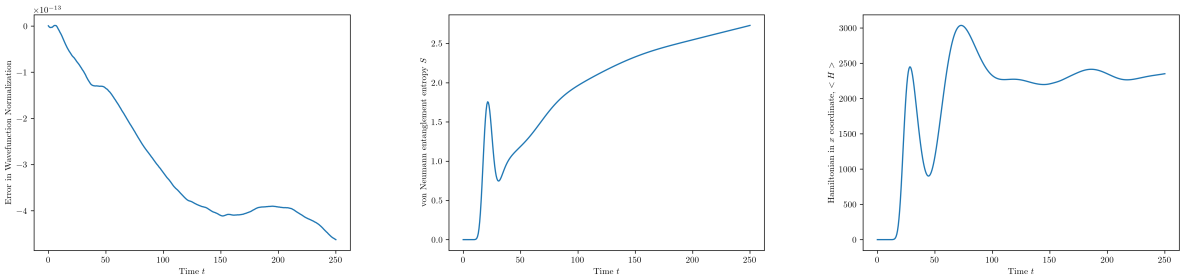

FIG. 9: Normalization, Entropy, and Hamiltonian of the 100x5000x1000 test with non-gound state initial Gaussian conditions.

D. Meeting Variables

For this section, I will use a series of variables agreed upon in the June 11 meeting, those being:

- $x \in [-5, 5], m = 100$
- $y \in [-25, 25], n = 5000$
- $t \in [0, 100], N = 1000$
- $x_0 = 0, y_0 = 10$
- $v_x = 0, v_y = -1$
- $\sigma_y = 3$
- $\lambda = 1$

This produced the following graphs:

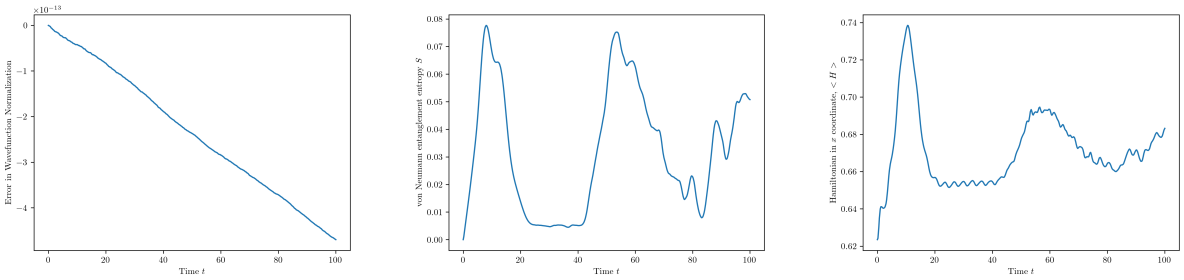

FIG. 10: Normalization, Entropy, and Hamiltonian of the 100x5000x1000 test with ground-state initial conditions and meeting-agreed-upon parameters.

The actual behaviour of the wave can be best described as a slow reflection upon the $y = 0$ point, then later a reflection upon the top of the boundary, and finally another reflection upon the $y = 0$ point. The jumps in entropy both happen at the reflection upon $y = 0$.

E. Expected Value Test 100x500x1000

The following results are similar to those above, as follows:

- $x \in [-5, 5], m = 100$
- $y \in [-5, 45], n = 500$

- $t \in [0, 40], N = 1000$
- $x_0 = 0, y_0 = 20$
- $v_x = 0, v_y = -1$
- $\sigma_y = 3$
- $\lambda = 1$

For the usual 3 plots, we get

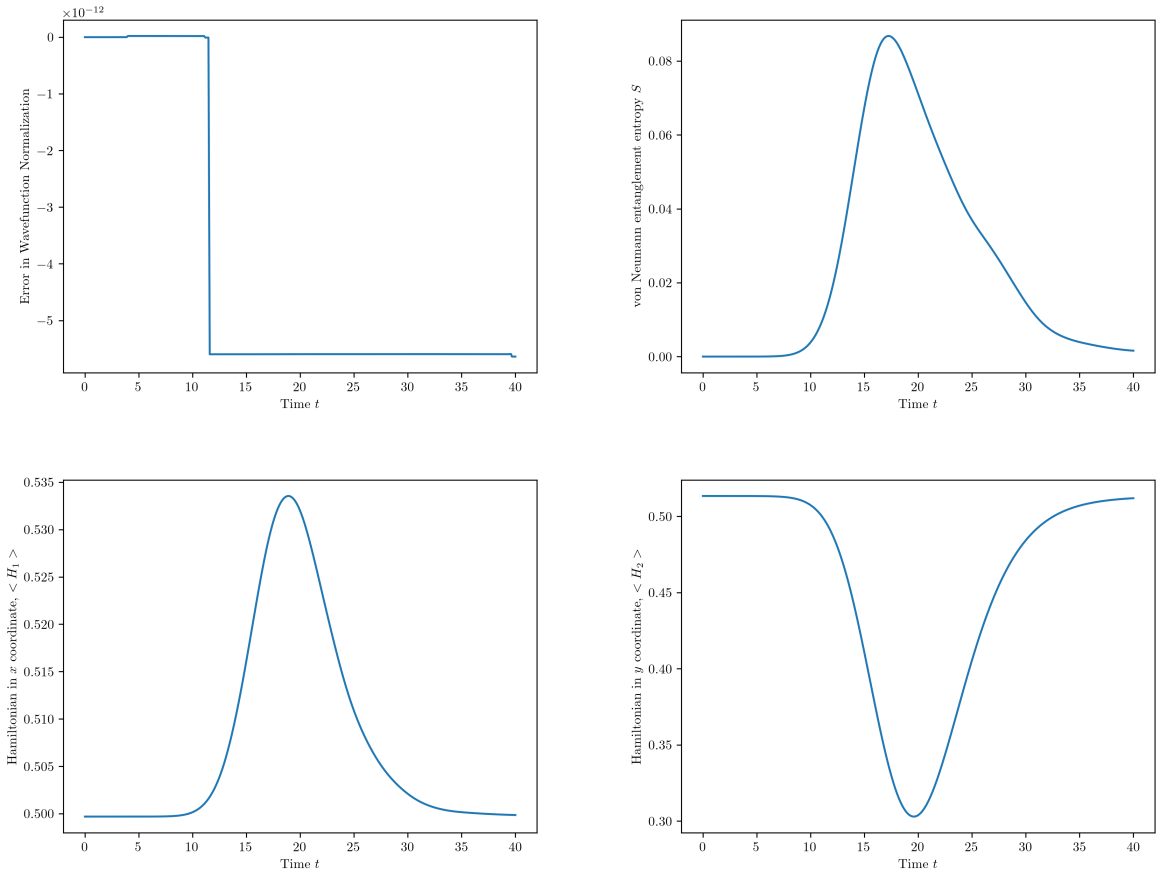

FIG. 11: Normalization, Entropy, and the x and y Hamiltonians respectively of the 100x500x1000 test with ground-state initial conditions and parameters above.

Furthermore, this gives the following expected values for $< x >$ and $< y >$:

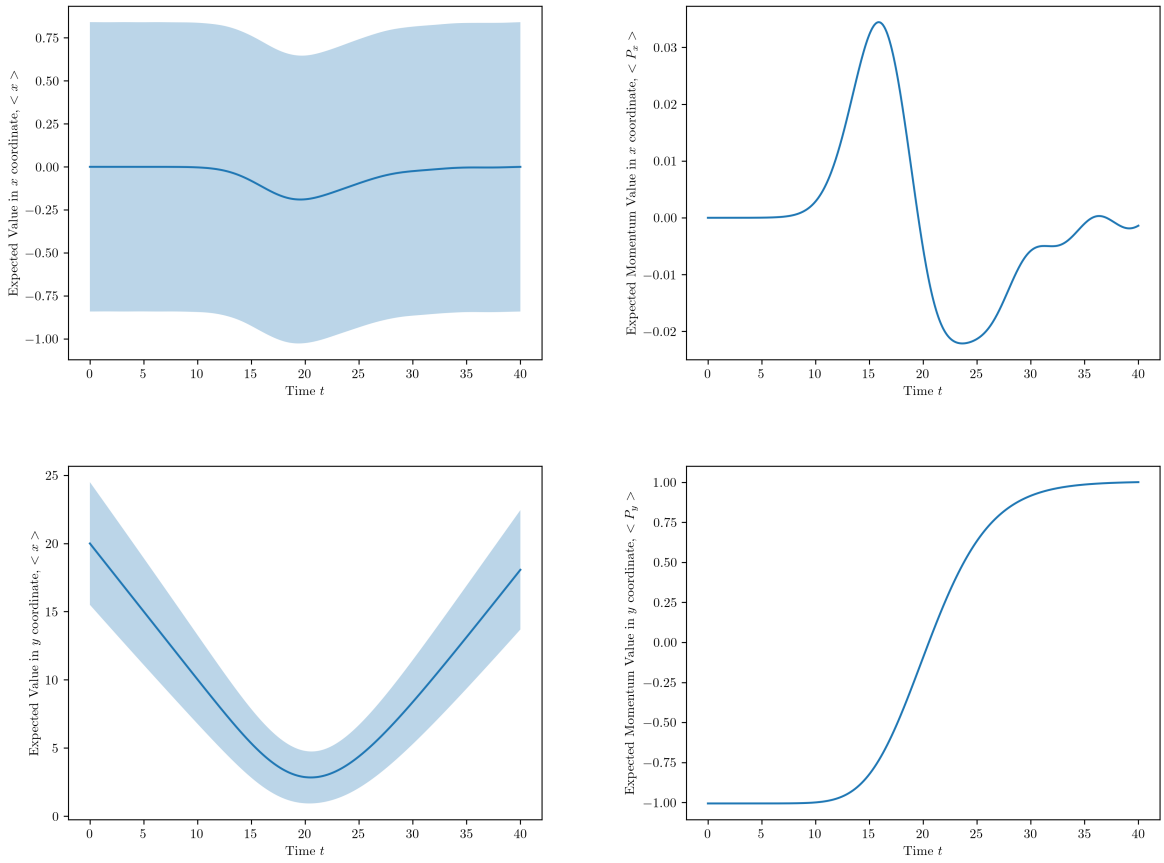

FIG. 12: Expected values for x, p_x, y, and p_y for this situation with $\sqrt{x}$ and $\sqrt{y}$ error regions for the position values.